Crystallization Region, Crystal Growth, and Characterization of Rubidium Titanyl Phosphate Codoped with Niobium and Lanthanide Ions

J. J. Carvajal, V. Nikolov,† R. Solé, Jna. Gavaldà, J. Massons, M. Aguiló, and F. Díaz*

Física i Cristal·lografia de Materials (FiCMA) and IEA, Universitat Rovira i Virgili, 43005 Tarragona, Spain

Received February 7, 2002. Revised Manuscript Received May 13, 2002

We studied the crystallization region of $RbTiOPO_4$ (RTP) codoped with Nb and Ln (Ln = Er^{3+} or Yb^{3+}), taking as basis a range of molar ratios of $Rb_2O-P_2O_5-TiO_2$. Significant differences in the critical concentration of Nb_2O_5 and Ln_2O_3 when we substituted TiO_2 with these oxides where observed. These differences depended on the initial molar ratio of $Rb_2O-P_2O_5-TiO_2$ used in each case. The critical concentrations of the two lanthanides were also different; the critical concentration of Yb_2O_3 was lower than that of Er_2O_3 for all compositions. The distribution coefficients and concentration of Ln in the crystals were higher for Yb^{3+} than for Er^{3+}, comparing similar concentrations in the solution. Single crystals of RTP:(Nb,Er) and RTP:(Nb,Yb) were grown with optical quality, and these were large enough to make spectroscopic characterizations.

Introduction

$KTiOPO_4$ (KTP) crystals and some of its isostructural materials have good nonlinear optical properties, which make them attractive for use as frequency doublers for diode lasers in the IR region.[1]

Doping these crystals with lanthanide ions (Ln) is interesting because the ion photoluminescence and the NLO properties of the matrix can be merged to achieve self-induced effects. Attempts to dope KTP crystals with Ln have been made but distribution coefficients have been very low.[2] Codopants generally increase the distribution coefficients of the lanthanide ions. In previous works, we showed that the use of Nb is one of the most effective ways of increasing these distribution coefficients, but the Ln concentrations so far achieved in KTP are too low to obtain efficient fluorescence from the REs.[2,3] Other attempts to improve these distribution coefficients have been made by completely substituting K^+ with Rb^+ to $RbTiOPO_4$ (RTP), but the distribution coefficients of Ln were still low.[3] Merging the effects of Rb^+ and Nb^{5+}, we achieved an Er^{3+} concentration of 0.65×10^{20} atoms·cm^{-3} and an Yb^{3+} concentration of 1.95×10^{20} atoms·cm^{-3}, but the NLO properties of the crystals are maintained.[4,5]

RTP crystallizes in the orthorhombic system, with the space group of symmetry $Pna2_1$. The cell parameters are $a = 12.974(2)$, $b = 6.494(3)$, and $c = 10.564(6)$ Å and $Z = 8$.[6] In a previous work, we determined the crystallization region of RTP in the ternary system $Rb_2O-P_2O_5-TiO_2$.[4] We also did some growth experiments of RTP:(Nb,Er) crystals for a fixed concentration of Nb and Er in the solution and several solution compositions in this crystallization region. Growth parameters, such as how fast the crystals grow, how efficient the crystal growth process is, and how much Er^{3+} is incorporated into the crystals, were significantly different and depended on the solution composition.[4] To better understand why this is so, a more detailed study of the crystallization region of RTP:(Nb,Ln) is needed.

In the present paper, we carried out the research of the crystallization region of RTP codoped with Nb^{5+} and Ln, particularly for Ln = Er^{3+} or Yb^{3+}. These ions are interesting because of their much-studied emissions around 1.5 μm from Er^{3+} and 1 μm from Yb^{3+} in different matrixes.[7] Er^{3+} is used in applications as optical communications at long distances due to its efficient emission near the region of optical losses in silica fibers (1.5 μm).[8] It is also used in medicine because of its emission at around 2.8 μm.[9] Yb^{3+} shows a simple scheme of levels with only two 4f electronic states that are optical accessible: the $^2F_{7/2}$ ground state and the $^2F_{5/2}$ excited state separated by an energy of around 10 000 cm^{-1}, which are split by the crystal field. This

* Corresponding author. E-mail: diaz@quimica.urv.es.
† Permanent address: Institute of General and Inorganic Chemistry, Bulgarian Academy of Sciences, 1040 Sofia, Bulgaria.

(1) Jacco, J. C.; Loiacono, G. M. *Appl. Phys. Lett.* **1991**, *58*, 560.
(2) Solé, R.; Nikolov, V.; Koseva, I.; Peshev, P.; Ruiz, X.; Zaldo, C.; Martín, M. J.; Aguiló, M.; Díaz, F. *Chem. Mater.* **1997**, *9*, 2745.
(3) Rico, M.; Zaldo, C.; Massons, J.; Díaz, F. *J. Phys. Condens. Matter* **1998**, *10*, 10101.
(4) Carvajal, J. J.; Nikolov, V.; Solé, R.; Gavaldà, Jna.; Massons, J.; Rico, M.; Zaldo, C.; Aguiló, M.; Díaz, F. *Chem. Mater.* **2000**, *12*, 3171.
(5) Carvajal, J. J.; Solé, R.; Gavaldà, Jna.; Massons, J.; Rico, M.; Zaldo, C.; Aguiló, M.; Díaz, F. *J. Alloys Compd.* **2001**, *323*−*324*, 231.
(6) Thomas, P. A.; Mayo, S. C.; Watts, B. E. *Acta Crystallogr.* **1992**, *B48*, 401.
(7) Kaminskii, A. A. *Crystalline Lasers: Physical Processes and Operating Schemes*; CRC Press: Boca Raton, FL, 1996.
(8) Dominiak-Dzik, G.; Golab, S.; Pracka, I.; Ryba-Romanowski, W. *Appl. Phys. A* **1994**, *58*, 551.
(9) Pujol, M. C.; Rico, M.; Zaldo, C.; Solé, R.; Nikolov, V.; Solans, X.; Aguiló, M.; Díaz, F. *Appl. Phys. B* **1999**, *68*, 187.

10.1021/cm0200745 CCC: $22.00
Published on Web 06/25/2002

energy matches the energy emitted by diode lasers very well. The ytterbium-doped lasers are also characterized by having a substantial long radiative lifetime, which makes pumping more efficient.[10] The emission around 1 μm from Yb^{3+} is particularly interesting in our case because it may be possible to double its frequency and so obtain a visible green radiation.

Finally, we grew single crystals of RTP:(Nb,Er) and RTP:(Nb,Yb) to analyze the crystal growth conditions and make a preliminary spectroscopic characterization, as promising new self-doubling materials.

Experimental Section

RTP Crystallization Regions. RTP melts incongruently in air around 1443 K.[11] Normal melt processes cannot therefore be used for crystal growth with RTP. In this paper, we used a high-temperature flux method. Taking as basis different molar ratios of $Rb_2O-P_2O_5-TiO_2$, the concentration of TiO_2 was progressively substituted with Nb_2O_5, Er_2O_3, or Yb_2O_3 or combinations of Nb_2O_5 and Er_2O_3 or Nb_2O_5 and Yb_2O_3 until the RTP phase disappeared and a new phase crystallized. We used Rb_2CO_3, $NH_4H_2PO_4$, TiO_2, Nb_2O_5, Er_2O_3, and Yb_2O_3 (p.a.) as initial reagents that we mixed at the desired ratios and decomposed by heating them until the bubbling of NH_3, H_2O, and CO_2 was complete. The solutions were prepared in 25 cm^3 platinum crucibles filled with 15−20 g of solution. The solutions were homogenized by maintaining them at a temperature of about 50−100 K above the expected saturation temperature for 3−5 h. The axial temperature gradient in the solution was 8 K, hot bottom. We decreased the temperature of the homogeneous solution at a rate of 10 K every 30 min until spontaneous crystallization appeared on a platinum wire immersed in the solution. The crystallized phases were identified by X-ray powder diffraction analysis and electron probe microanalysis (EPMA), and the morphology of the crystals was observed by optical and scanning electron microscopies. The variation of the RTP crystallization region was obtained after studying around 20−50 solution compositions, depending on the initial molar ratio of $Rb_2O-P_2O_5-TiO_2$.

Top-Seeded Solution Growth (TSSG). Then, we grew RTP:(Nb,Er) and RTP:(Nb,Yb) single crystals by the TSSG slow-cooling technique using a vertical tubular furnace controlled by a Eurotherm 818P controller/programmer. The solution, which weighed 30−40 g, was prepared as before. The axial temperature gradient in the solution was about 10 K, hot bottom. The crystals were grown on oriented RTP seeds with the *c* crystallographic direction perpendicular to the surface of the solution, displaced 4−5 mm from the rotation axis, and fixed in a growth device that included a platinum turbine to additionally stir the solution.[4] The *a* direction of the two seeds used in every growth experiment was always placed in the radial direction of the rotation movement. We determined the saturation temperature from the growth or dissolution of the seeds in contact with the surface of the solution. During the growth processes, we reduced the temperature by 12 K from the temperature of saturation at a rate of 1 $K \cdot day^{-1}$. The rotation was kept constant at 65 rpm in all experiments. When the growth process was complete, we slowly removed the crystals from the solution to minimize any thermal stress and kept them above the surface of the solution, while the temperature of the furnace was lowered to room temperature at a rate of 15 $K \cdot h^{-1}$.

Dopant Concentration Analyses. The concentration of dopants was analyzed by EPMA operating in wavelength-dispersive mode. An electron microprobe CAMECA SX-50 was used in the analyses. The samples were included in a polyester ortoftalic-type resin forming cylinders of 2.5 cm in diameter and 1 cm in high. The surfaces of the samples were polished with diamond powders until a grain size of 1 μm, using a Struers DAP-7 polisher. The surface of the cylinder was cleaned with ethanol and was sputtered with carbon before taking the measurements. The concentrations of Rb, Ti, P, Nb, and O were analyzed at 30 nA electron current and those of Er and Yb at 100 nA. The accelerating voltage was kept at 25 kV in all cases. A pure RTP crystal, grown by ourselves, was used as standard for Rb, Ti, P, and O in aim to minimize the matrix effects in the samples because of its similar chemical composition. The other standards were $LiNbO_3$ for Nb, REE1 (a synthetic glass with a base of Si−Al−Ca and a concentration of 4.09% of Er in weight) for Er, and YbF_3 for Yb. The analyses were made using the lines Rb Lα and P Kα measured with the TAP crystal, Ti Kα and Nb Lα measured with the PET crystal, O Kα measured with a W/Si ($2d$ = 60 Å) multilayer crystal, and finally Er Lα and Yb Lα measured with the LiF crystal. The measurements were integrated during 10 s for Rb, Ti, P, and O and 30 s for Nb, Er, and Yb. The raw intensities were corrected for dead time, background, and matrix effects using the PAP correction procedure.[12]

Optical Absorption. Optical absorption of Er^{3+} and Yb^{3+} was performed in RTP:(Nb,Er) and RTP:(Nb,Yb) crystals with a Varian Cary 500 Scan spectrophotometer. Because of the anisotropy of the crystal, these measurements were performed using incident light polarized parallel to the three crystallographic directions of the crystals, which, as RTP crystallizes in the orthorhombic system, coincide with the three principal optical axes. The spectra were collected at room temperature in the 350−1750 nm range for samples containing Er^{3+} and in the 800−1100 nm range for samples containing Yb^{3+}.

We prepared the samples by cutting the crystals to form 2-mm thick square prisms parallel to the (100), (010), and (001) planes and polishing them to optical quality using alumina powder.

Results and Discussion

RTP Crystallization Regions. We chose two basic molar ratios of $Rb_2O-P_2O_5-TiO_2$ to study how the crystallization region of RTP and the distribution coefficients of dopants vary when TiO_2 is substituted by Nb_2O_5 and Ln_2O_3 in the solution. These molar ratios were $Rb_2O-P_2O_5-TiO_2$ = 43.1−31.9−25.0 and 40.8−27.2−32.0, respectively.

Figures 1−4 show the change in the crystallization region of RTP when some of the TiO_2 in the solution was substituted by Nb_2O_5 and Er_2O_3 or Nb_2O_5 and Yb_2O_3. These concentrations were defined as

$$\langle Nb_2O_5 \rangle = \frac{[Nb_2O_5]}{[TiO_2] + [Nb_2O_5] + [Ln_2O_3]}$$

and

$$\langle Ln_2O_3 \rangle = \frac{[Ln_2O_3]}{[TiO_2] + [Nb_2O_5] + [Ln_2O_3]}$$

where Ln = Er or Yb. In these figures, we can see the critical concentration of dopants that substituted TiO_2 in solution, below which the RTP phase crystallized and above which other phases appeared. This is a very important parameter for growing RTP:(Nb,Ln) crystals. As the solution was poorer in Rb_2O and P_2O_5 and richer in TiO_2, the critical concentration of Nb decreased, whereas the critical concentration of Ln increased. The critical concentration of Nb ranged from 9 mol % for a

(10) Wang, P.; Dawes, J. M.; Deckker, P.; Knowles, D. S.; Piper, J. A. *J. Opt. Soc. Am. B* **1999**, *16*, 63.

(11) Cheng, L. K.; Bierlein, J. D.; Ballman, A. A. *J. Cryst. Growth* **1991**, *110*, 697.

(12) Pouchou, J. L.; Pichoir, F. *Rech. Aerosp.* **1984**, *3*, 13.

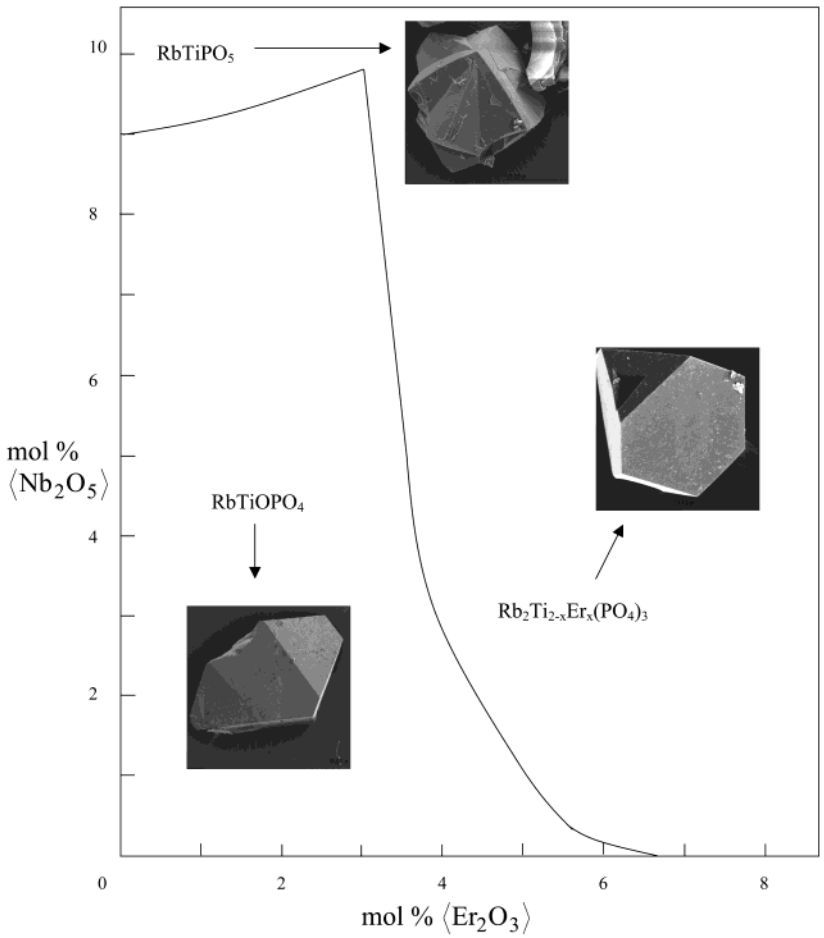

Figure 1. Variation of the crystallization region of RTP with the substitution of TiO_2 by Nb_2O_5 and Er_2O_3, taking as basis a solution with a molar composition $Rb_2O-P_2O_5-(TiO_2 + Nb_2O_5 + Er_2O_3) = 43.1-31.9-25.0$. SEM images of RTP and the neighboring phases.

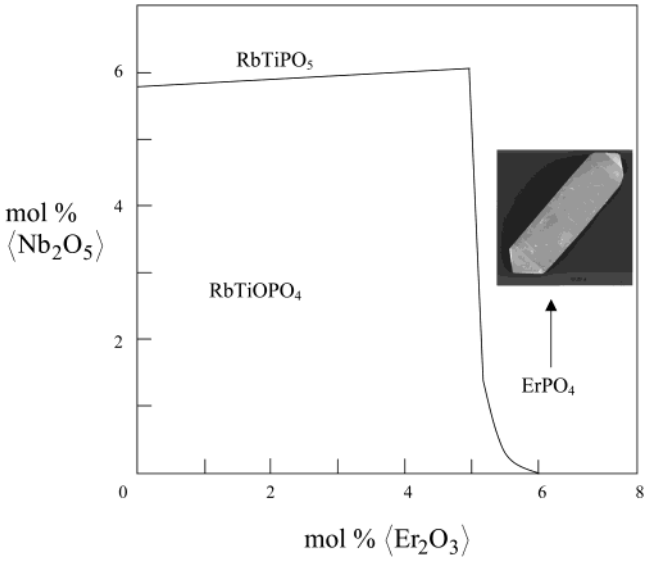

Figure 2. Variation of the crystallization region of RTP with the substitution of TiO_2 by Nb_2O_5 and Er_2O_3, taking as basis a solution with a molar composition $Rb_2O-P_2O_5-(TiO_2 + Nb_2O_5 + Er_2O_3) = 40.8-27.2-32.0$. SEM images of the neighboring phases.

initial solution containing 25 mol % of TiO_2 to 5.5 mol % when the solution contained 32 mol % of TiO_2. If we compare the two Ln, we can see that, when the solution composition is equal and the solution is poor in TiO_2, the critical concentration of Er_2O_3 is higher than that of Yb_2O_3. However, when the concentration of TiO_2 in the initial solution is richer, the critical concentration of Er_2O_3 is lower than that of Yb_2O_3. To be exact, when the initial solution was formed by $Rb_2O-P_2O_5-TiO_2 = 43.1-31.9-25.0$, the critical concentration of Er_2O_3 in the solution, in which TiO_2 was substituted for, was 6 mol %, whereas the concentration of Yb_2O_3 in the same conditions was only 3 mol %. However, when the initial solution contained $Rb_2O-P_2O_5-TiO_2 = 40.8-27.2-32.0$, these critical concentrations increased to 6 mol % for Er_2O_3 and over 8 mol % for Yb_2O_3.

We have identified several new phases in the boundary of the RTP crystallization regions in these systems. When the critical concentration of Nb_2O_5 is exceeded (see Figures 1−4), $RbTiPO_5$ phase doped with Nb was observed. In solutions with a low content in TiO_2, when the critical concentration of Ln_2O_3 is overpassed, $Rb_2Ti_{2-x}Ln_x(PO_4)_3$ was identified, as can be seen in Figures 1 and 3. In solutions with a richer content in TiO_2, we have identified different neighboring phases of the crystallization region of RTP depending on the Ln used. When the critical concentration of Er_2O_3 was exceeded, we detected the presence of $ErPO_4$ (see Figure 2). When the concentration of Yb_2O_3 was above the critical concentration, we identified $Rb_3Yb_2(PO_4)_3$ (see Figure 4). These phases were identified by EPMA and X-ray powder diffraction, and the SEM images of all of them can be seen in Figures 1−4.

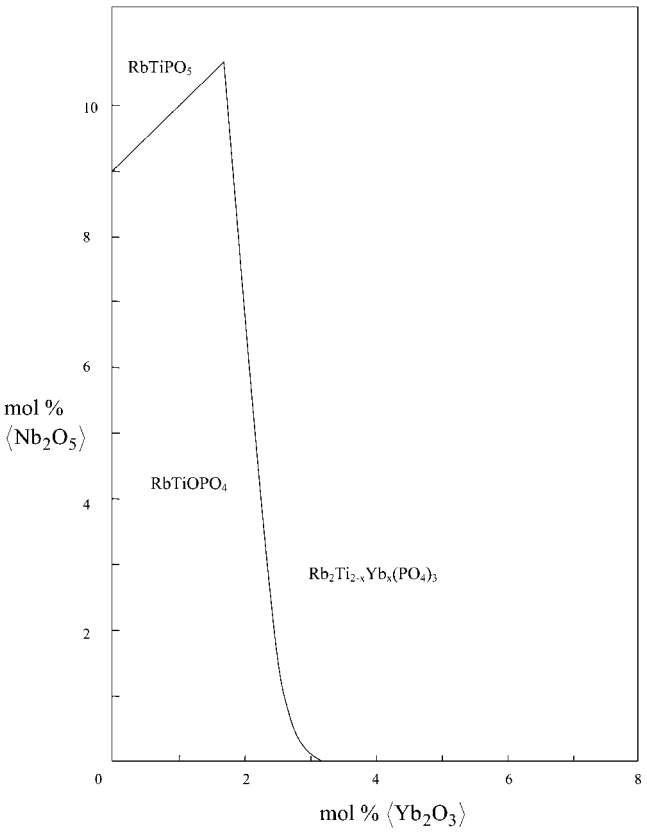

Figure 3. Variation of the crystallization region of RTP with the substitution of TiO_2 by Nb_2O_5 and Yb_2O_3, taking as basis a solution with a molar composition $Rb_2O-P_2O_5-(TiO_2 + Nb_2O_5 + Yb_2O_3) = 43.1-31.9-25.0$.

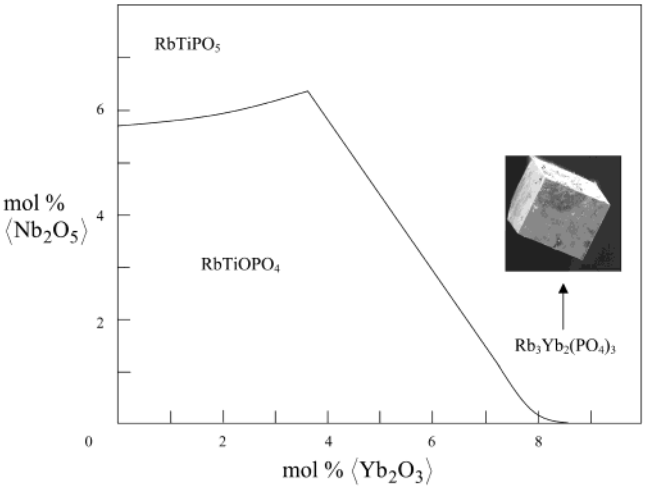

Figure 4. Variation of the crystallization region of RTP with the substitution of TiO_2 by Nb_2O_5 and Yb_2O_3, taking as basis a solution with a molar composition $Rb_2O-P_2O_5-(TiO_2 + Nb_2O_5 + Yb_2O_3) = 40.8-27.2-32.0$. SEM images of the neighboring phases.

The most significant differences were in the distribution coefficients of these ions in the crystallization regions we studied. The distribution coefficients were defined as

$$K_{DE} = \frac{\left\{\frac{[DE]}{[Ti]+[Nb]+[Ln]}\right\}_{crystal}}{\left\{\frac{[DE]}{[Ti]+[Nb]+[Ln]}\right\}_{solution}}$$

Table 1. Distribution Coefficients of Er^{3+} (K_{Er} = Upper Value) and Nb^{5+} (K_{Nb} = Lower Value) in RTP:(Nb,Er) Crystals Using a Molar Solution Composition of $Rb_2O-P_2O_5-(TiO_2 + Nb_2O_5 + Er_2O_3) = 43.1-31.9-25.0$[a]

	mol % ⟨Er_2O_3⟩				
mol % ⟨Nb_2O_5⟩	0	1	2	3	4
0			0.03		0.04
			–		–
2	–	0.20	0.13	0.11	0.14
	0.83	0.78	0.78	0.77	0.86
4	–		0.15		
	0.72		0.64		
6	–		0.18	0.16	
	0.67		0.56	0.69	
8	–		0.11	0.15	
	0.57		0.47	0.44	
9				0.15	
				0.50	

[a] (–) No value.

Table 2. Distribution Coefficients of Er^{3+} (K_{Er} = Upper Value) and Nb^{5+} (K_{Nb} = Lower Value) in RTP:(Nb,Er) Crystals Using a Molar Solution Composition of $Rb_2O-P_2O_5-(TiO_2 + Nb_2O_5 + Er_2O_3) = 40.8-27.2-32.0$[a]

	mol % ⟨Er_2O_3⟩			
mol % ⟨Nb_2O_5⟩	0	2	4	5
0		0.11	0.07	
		–	–	
2	–	0.46	0.33	0.24
	0.80	0.99	1.13	0.90
4	–	0.36	0.31	0.23
	0.45	0.69	0.62	0.56
6		0.41	0.23	
		0.53	0.45	

[a] (–) No value.

Table 3. Distribution Coefficients of Yb^{3+} (K_{Yb} = Upper Value) and Nb^{5+} (K_{Nb} = Lower Value) in RTP:(Nb,Yb) Crystals Using a Molar Solution Composition of $Rb_2O-P_2O_5-(TiO_2 + Nb_2O_5 + Yb_2O_3) = 43.1-31.9-25.0$[a]

	mol % ⟨Yb_2O_3⟩			
mol % ⟨Nb_2O_5⟩	0	1	2	3
0			0.07	
			–	
2	–		0.30	
	0.83		0.85	
4	–	0.39	0.35	
	0.72	0.75	0.69	
6	–	0.37	0.35	0.23
	0.67	0.71	0.63	0.52
8	–	0.36	0.38	
	0.57	0.57	0.54	
9		0.30		
		0.51		

[a] (–) No value.

where DE = Nb, Er, or Yb and Ln = Er or Yb. These distribution coefficients are listed in Tables 1–4 in the relation of ⟨Ln_2O_3⟩ and ⟨Nb_2O_5⟩.

The distribution coefficient of Ln increased as the concentration of Nb_2O_5 increased up to a maximum of around 4–6 mol %, depending of composition of the initial solution. After that, the distribution coefficient of Ln decreased, except for Er in $Rb_2O-P_2O_5-TiO_2 = 40.8-27.2-32.0$, where the distribution coefficient of Er decreased when the concentration of Nb_2O_5 was 2 mol % or more. This decrease in the distribution coefficient of Ln can be due to a competition mechanism between the Ln and Nb ions, because both Ln and Nb are expected to substitute Ti in the structure. Therefore, as

Table 4. Distribution Coefficients of Yb^{3+} (K_{Yb} = Upper Value) and Nb^{5+} (K_{Nb} = Lower Value) in RTP:(Nb,Yb) Crystals Using a Molar Solution Composition of $Rb_2O-P_2O_5-(TiO_2 + Nb_2O_5 + Yb_2O_3) = 40.8-27.2-32.0$[a]

	mol % ⟨Yb_2O_3⟩					
mol % ⟨Nb_2O_5⟩	0	2	3	4	5	6
0		0.08	0.08	0.14	0.11	
		−	−	−	−	
1	−	0.30	0.39	0.30	0.28	0.20
	0.88	0.80	1.00	1.11	1.18	1.16
2	−	0.56	0.54	0.42		0.28
	0.80	1.05	0.93	0.92		1.01
3	−	0.96	0.59	0.31	0.39	0.33
	0.51	0.94	0.94	0.76	0.88	0.98
4	−	0.55	0.64	0.52	0.42	
	0.45	0.88	0.80	0.82	0.78	
5	−	0.62	0.64	1.14	0.46	
	0.57	0.64	0.65	0.79	0.75	
6		0.56	0.59			
		0.49	0.52			
7			0.62			
			0.58			

[a] (−) No value.

the Nb is smaller than the Ln ion (Nb^{5+} has an ionic radius of 0.680 Å and Ln^{3+} has one of about 0.9 Å, both for an octahedrical environment),[13] the mobility of Nb is higher and, also due to its radius is closer to that of Ti^{4+}, the probability that this ion occupies the positions of Ti is greater. This mechanism is confirmed by the fact that, when the concentration of Nb in the solution is increased, its distribution coefficient in the crystal is decreased because Nb cannot totally substitute Ti in the structure and there are not enough free places that can be occupied by Nb. We could find no rule to explain how the distribution coefficient of Ln changed as the concentration of Ln changed. Some values of the distribution coefficients in the areas close to the boundary phases are irregular because more than one phase crystallizes at these points. This could change the real concentration of Nb and Ln in the solution.

The fact that the distribution coefficients of Yb were higher than those of Er (see Tables 1 and 3 or Tables 2 and 4) could be explained in terms of ionic radii. In an octahedrical environment, Er^{3+} has an ionic radius of 0.890 Å and Yb^{3+} one of 0.868 Å, which is closer to that of Ti^{4+} (0.605 Å).[13] If Ln substitutes Ti^{4+} in the structure, the ions whose ionic radius is closer to that of Ti^{4+} have a greater tendency to incorporate into the crystals and, therefore, have larger distribution coefficients.

The distribution coefficient of Er and Yb also increased when the initial solution contained a higher concentration of TiO_2 and a higher relation Rb_2O/P_2O_5 (see Tables 1 and 2 and Tables 3 and 4). The distribution coefficient of Yb^{3+} in a solution with a molar ratio of $Rb_2O-P_2O_5-TiO_2$ equal to 40.8−27.2−32.0 was at least twice than that obtained in a solution formed by a molar ratio $Rb_2O-P_2O_5-TiO_2$ = 43.1−31.9−25.0. This effect is difficult to explain. Our suposition is that the viscosity of the solution is higher when the ratio Rb_2O/P_2O_5 decreases, taking into acount a similar behavior than that observed in self-flux solutions of KTP.[14] So, if the solution is more viscous, the mobility of the ions is more difficult and they tend to be less to incorporated into the crystal. The high viscosity of the solution works against its homogeneity, producing a lack of mixing and the difficulty that the Ln could form structural units that could be incorporated into the crystal growing. Other parameters, such as the temperature of solution, must also be taken into account to explain this effect, however. When the concentration of TiO_2 in the solution is higher, the saturation temperature increased, and at higher temperatures, the structure is more expanded and Ln can enter the structure more easily. Other parameters that can contribute to this effect are the speed at which crystals grow, the diffusion coefficient, and how far the growth conditions are from the equilibrium thermodynamic conditions.

The distribution coefficients of Nb were higher that those of the Ln, because its ionic radius is closer to that of Ti^{4+}.[13] We have observed that K_{Nb} decreased as the concentration of Nb_2O_5 increased. How this distribution coefficient changed as the concentration of Ln_2O_3 changed did not follow a clear pattern (see Tables 1−4). When the solution was richer in TiO_2 and the relation of Rb_2O/P_2O_5 was greater, the distribution coefficients of Nb were lower if the solution did not contain Ln_2O_3. This behavior changed, however, when Ln_2O_3 was added to the solution and distribution coefficients of Nb tended to be higher, as can be seen in Tables 2 and 4. This effect can be explained by the reciprocal action of Nb upon the Ln ions. As we have seen, the presence of Nb in the crystals improves the distribution coefficient of Ln but, to a lesser extent, this Ln also improves the distribution coefficient of Nb in the crystals.

TSSG of RTP:(Nb,Ln) Crystals. We grew RTP:(Nb,Ln) crystals with Ln = Er or Yb by the TSSG slow-cooling technique. In these experiments, we kept the rate of cooling, the interval of decrease in temperature, and the speed of rotation of the growth system constant.

The crystals grown show the previously described morphology:[4,5] the (100) face becomes the most devel-

Table 5. Growth Data Associated with RTP:(Nb,Ln) Single Crystals

expt no.	solution composition (mol %) $Rb_2O/P_2O_5/TiO_2/Nb_2O_5/Er_2O_3/Yb_2O_3$	soln wt (g)	$\Delta T_{saturation}$ (K)	efficiency (%)	crystal dimensions ($a \times b \times c$) (mm)	crystal wt (g)	avg supersaturation (g/K × 100 g of solution)	K_{Nb}	K_{Er}	K_{Yb}
1	42.9/35.1/20.9/0.66/0.44/0	29.5	4	50	2.1 × 5.5 × 5.2 2.2 × 5 × 4.5	0.260	0.122	0.57	0.04	
2	41.2/33.7/23.7/0.75/0.5/0	37	6.5	59	2.5 × 5 × 5 2.7 × 4.5 × 4.5	0.237	0.099	0.62	0.04	
3	44.4/29.6/24.7/0.78/0.52/0	26	1	8	1.6 × 1.4 × 1.4 1.6 × 3 × 1.4	0.024	0.092	0.26	0.06	
4	42.0/28.0/28.5/0.9/0.6/0	28	1.5	12	2.4 × 2.3 × 2.8 1.9 × 1.9 × 2.1	0.040	0.095	0.37	0.14	
5	40.8/27.2/30.0/1.0/0/1.0	41.6	3.5	29	1.8 × 3.7 × 3.7 1.7 × 3.2 × 3.5	0.08	0.055	0.60		0.50
6	40.8/27.2/30.1/0.6/0/1.3	42.1			3.7 × 13.0 × 7.5	0.640		0.75		0.21

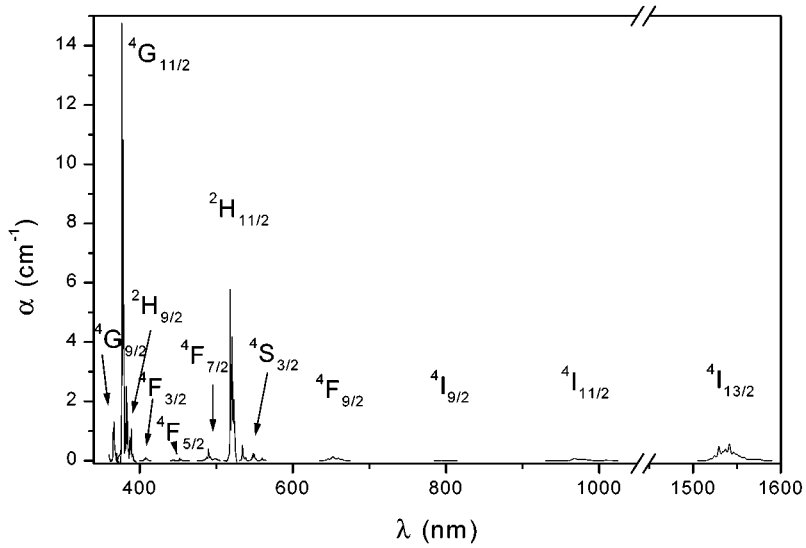

Figure 5. Optical absorption of Er^{3+} in RTP:(Nb,Er) at room temperature using incident polarized light parallel to the *c* crystallographic axis. All observed transitions start from the $^4I_{15/2}$ ground state.

oped face in the crystal and the crystals take on the appearance of plates. Another aspect are the cracks starting from the RTP seed. For KTP crystals, this problem was solved using KTP:Nb seeds,[15] but our results seem to show that these defects cannot be fully prevented using RTP:Nb seeds.

Significant differences in parameters such as efficiency, crystal size, weight of the crystals, and distribution coefficients of the dopant ions have been observed. Efficiency is defined as

$$\text{efficiency} = \left[\frac{T_s - T_s'}{T_s - T_{final}}\right] \times 100$$

where T_s is the saturation temperature before the growth process, T_s' is the saturation temperature after the growth process, and $(T_s - T_{final})$ is the total temperature decrease during the growth process. All of these results are shown in Table 5. Other parameters also given in Table 5 are the difference in the saturation temperature, $\Delta T_s = T_s - T_s'$, and the average of supersaturation, defined as avg supersaturation = [cryst wt/($\Delta T_s \times$ solution wt)] $\times$ 100, in addition to the growth conditions used.

The distribution coefficients of the Ln in these crystals are slightly lower than when we calculated them with crystals grown on a Pt rod, without seeds, when we studied the corresponding crystallization region. This may be due to the additional stirring of the solution used in the growth experiments,[4] which improves homogeneity and mass transport efficiency in the solution, and to the different rate of cooling and, therefore, to the different growth velocity.

As Table 5 shows, crystals grown in a solution with a lower concentration of Nb_2O_5 were larger than those grown in solutions with a higher concentration of Nb_2O_5. However, the distribution coefficient of Ln ion in these crystals was lower. Then, the presence of Nb in the solution clearly enhances the distribution coefficient of Ln but strongly affects the growth mechanism of the RTP crystals. In another way, experiments 1 and 2, with a higher molar relation Rb_2O/P_2O_5, were more efficient. The average of supersaturation was similar for all experiments to growth RTP:(Nb,Er) crystals, but this parameter seems to change in experiments to growth RTP:(Nb,Yb) crystals. This hypothesis cannot be confirmed, however, because it is difficult to grow these crystals with different concentration of Nb and Yb in

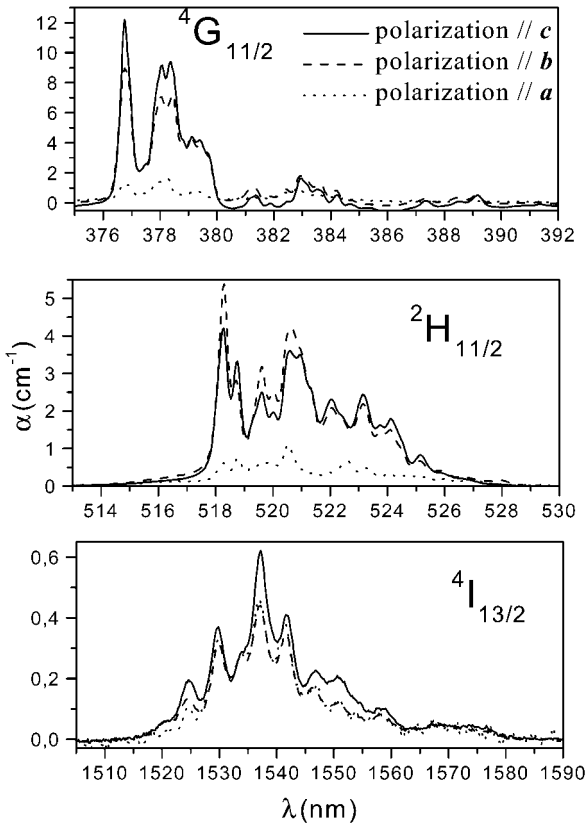

Figure 6. $^4G_{11/2}$, $^2H_{11/2}$, and $^4I_{13/2}$ multiplets of Er^{3+} in RTP:(Nb,Er) at room temperature using incident polarized light parallel to the three crystallographic axes. All observed transitions start from the $^4I_{15/2}$ ground state.

(13) Shannon, R. D. *Acta Crystallogr.* **1976**, *A32*, 751.
(14) Iliev, K.; Peshev, P.; Nikolov, V.; Koseva, I. *J. Cryst. Growth* **1990**, *100*, 225.
(15) Wang, J.; Liu, Y.; Jiang, M.; Shao, Z.; Liu, W.; Jiang, S. *Cryst. Res. Technol.* **1997**, *21*, 3319.

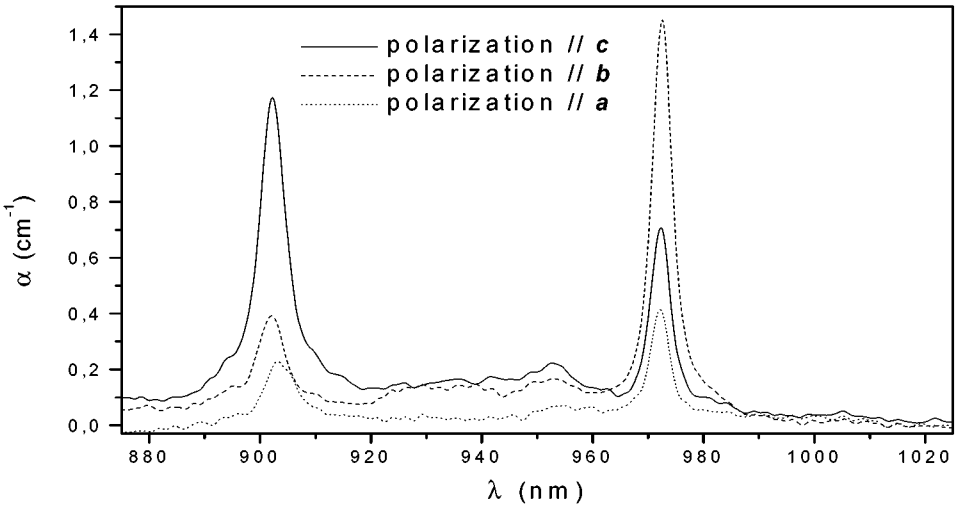

Figure 7. $^2F_{5/2}$ multiplet of Yb^{3+} in RTP:(Nb,Yb) at room temperature using incident polarized light parallel to the three crystallographic axes. The observed transition starts from the $^2F_{7/2}$ ground state.

the solution. This can be seen in experiment 6, where after many attempts only one crystal of poor quality was grown, despite the fact that two seeds were used as in the other experiments, and its quality is poor. Research to find the suitable conditions for growing RTP:(Nb,Yb) crystals is in progress.

Optical Absorption. Finally, we measured the absorption spectra of Er^{3+} and Yb^{3+} in the RTP:(Nb,Er) and RTP:(Nb,Yb) crystals using polarized light parallel to the three crystallographic axes of the crystal at room temperature because any measurement performed out of these directions will result in a composition of the optical absorption in the three principal optical axes. Figures 5−7 show the spectra studied. Twelve multiplets of Er^{3+} ($^4G_{9/2}$, $^4G_{11/2}$, $^2H_{9/2}$, $^4F_{3/2}$, $^4F_{5/2}$, $^4F_{7/2}$, $^2H_{11/2}$, $^4S_{3/2}$, $^4F_{9/2}$, $^4I_{9/2}$, $^4I_{11/2}$, and $^4I_{13/2}$) and the only multiplet of Yb^{3+} ($^2F_{5/2}$) were resolved. A strong dichroism was detected in the samples. For the crystals containing Er^{3+}, the intensities of the three spectra collected parallel to *a*, *b*, and *c* crystallographic directions were significantly different (Figure 6 shows the three most intense multiplets of Er^{3+} in greater detail). The same behavior was observed in the $^2F_{5/2}$ multiplet of Yb^{3+}, as can be seen in Figure 7. Although this manifold was observed in the three polarized spectra, the higher intensity was obtained in the spectra collected parallell to the *c* direction, followed by this one collected parallell to the *b* direction, and the spectra that shows a lower intensity is that collected parallell to the *a* direction. The use of a such dichroic material will support the advantages in the obtaining of polarized laser emissions.

Conclusions

The codoping of RTP crystals with Nb and Ln depended significantly on the composition of the solution used. The critical concentrations of Nb_2O_5, Er_2O_3, and Yb_2O_3 and the distribution coefficients of Nb^{5+}, Er^{3+}, and Yb^{3+} varied significantly. These differences were attributed to many factors, including the different ionic radii, the viscosity of the growth solution, the difussion coefficient, and the speed of growth. The distribution coefficient of Yb^{3+} was always higher than that of Er^{3+}. This may have been because their ionic radii are different. Several new boundary phases to these systems were identified: $RbTiPO_5$ doped with Nb, $Rb_2Ti_{2-x}Ln_x(PO_4)_3$ with Ln = Er and Yb, $ErPO_4$, and $Rb_3Yb_2(PO_4)_3$. Single crystals of RTP:(Nb,Er) and RTP:(Nb,Yb) of good optical quality were successfully grown and these were large enough to make latter characterizations such as absorption studies of the Ln^{3+} ions in this matrix. Spectroscopic studies showed that there was a strong dichroism in the intensities of the different multiplets of Er^{3+} and Yb^{3+} depending on the polarization of the incident light.

Acknowledgment. The authors thank Dr. X. Llovet of the Universitat de Barcelona for his helpful discussions in EPMA analyses. This work has been supported by CICyT under Projects MAT99-1077-C02 and FIT-070000-2001-477 and by CIRIT under Project 2001SGR 00317. J.J.C. also acknowledges the grant from the Catalonian Government (2000FI 00633 URV APTIND).

CM0200745